Available online at www.sciencedirect.com

ScienceDirect

Procedia CIRP 123 (2024) 404–409

www.elsevier.com/locate/procedia

7th CIRP Conference on Surface Integrity

Towards the numerical simulation of tool wear induced residual stress drift

F.Clavier[a], F.Valiorgue[a], C.Courbon[a,*], J.Rech[a], A.Van Robaeys[b], Y.Chen[c], J.Kolmacka[d], H.Karaouni[e]

[a] Univ Lyon, Ecole Centrale de Lyon, CNRS, ENTPE, LTDS, UMR5513, ENISE, 42023 Saint Etienne
[b] Airbus Helicopters, Aéroport Marseille Provence, 13725 Marignane, France
[c] CETIM, 52, avenue Félix-Louat, 60300 Senlis, France
[d] Framatome Centre Technique, B.P. 40 001 – Saint Marcel, 71328 Chalon sur Saône, France
[e] SAFRAN Tech, Rue des Jeunes-Bois, 78772 Magny-les-Hameaux, France

* Corresponding author. Tel.: +33 4 77 43 75 48. E-mail address: cedric.courbon@enise.ec-lyon.fr

Abstract

Finish turning is one of the key operations governing the residual stress of functional surfaces. The residual stress state is determined by the cutting conditions and the selected cutting tool system (macro geometry, cutting edge preparation, tool substrate, multi-layer coating…). However, this initial configuration evolves over time due to tool wear. Therefore, it seems fundamental to reproduce the wear process of the tool in order to understand the evolution of thermo-mechanical loadings applied to the machined surface. This work presents a numerical methodology for predicting the wear-induced residual stress drift in longitudinal turning. The complete 3D cutting tool is discretized into elementary 2D sections. A finite element based procedure is developed to calculate, considering each local tool geometry, the local loads withstood by the machined material. The latter are merged to generate equivalent 3D thermomechanical loadings implemented in a second macroscopic model able to calculate the residual stress state under different wear levels. Experimental cutting tests with artificially worn tools have confirmed that good agreement can be achieved.

Keywords: Tool wear; surface integrity; turning; numerical modelling; residual stress

1. Introduction

Several key sectors of industry place a strong emphasis on the fatigue resistance of safety components. The residual stress state near the functional surface, which plays a significant role, is known to be affected by machining processes during manufacturing [1–5].

Past studies have shown that residual stresses are greatly impacted by various parameters such as tool geometry [6,7] coating [8], cutting conditions [7,9,10] and material [9,11]. Additionally, tool wear has a significant impact on the residual stress gradient at the surface of a machined component. Several research works have shown that its effects can be completely different depending on the tool, workpiece material and cutting conditions [11–14], which makes general conclusions about its impact difficult to state.

Today, the challenge for the scientific community, but also industry, is no longer to predict the residual stress state but to evaluate its drift induced by unavoidable phenomena such as tool wear. This can be particularly critical when machining long components such as in aircraft or nuclear industry as this drift can occur all along the finished surface produced by a single cut.

Numerical simulation can be a valuable tool in addressing this problem, but modelling residual stress caused by a worn tool remains a key issue. Despite many studies observing the impact of a worn tool on thermomechanical loadings [15–17] only a few have focused on residual stress prediction [18,19]. These studies often use simplified 2D cutting configurations,

10.1016/j.procir.2024.05.071

which can provide good correlation between experimental and numerical results but are restrictive regarding the targeted industrial applications. It is thus necessary to consider the actual machining operation, the 3D geometry of the tool and the cyclic nature of the machining process to reliably predict such outputs [20].

While prediction models already exist for residual stresses, there is a clear need to develop a methodology taking into account the actual changes in tool geometry caused by wear such as flank wear, cutting edge radius, or local rake angle in a true 3D cutting configuration.

This study builds on several previous works and proposes a hybrid numerical modeling approach able to predict the impact of a worn cutting tool on residual stress distribution in a 3D longitudinal turning operation.

Nomenclature

$r\beta$	cutting edge radius
γ_n	rake angle
α_n	flank angle
λ_s	inclination angle
κ_r	orientation angle
v_c	cutting speed
f	feed rate
a_p	depth of cut
VB	flank wear length
α_{VB}	flank wear angle
$S(i)$	elementary 2D section
$h(i)$	local uncut chip thickness

2. Experimental setup

2.1. Investigated configuration

Longitudinal turning tests were performed on a 15-5 PH martensitic stainless steel (state H1025, hardness = 35HRC; tensile strength = 1070MPa; yield strength = 1000MPa).

DNMG 150608 inserts made of TiCN+Al2O3 coated cemented carbide with an initial cutting edge radius $r\beta$ of 70µm were employed. Once fitted on a PDJNL 2020K15 tool holder, it resulted in a rake angle γ_n of 1°, a clearance angle α_n of 6°, an inclination angle λ_s of 0° and an orientation angle κ_r of 93°.

The tests were conducted under dry conditions and with the following cutting parameters: a cutting speed v_c of 120m/min with a feed rate f of 0.2mm/rev and a depth of cut a_p of 0.2mm.

Residual stresses were assessed by the X-Ray diffraction method using an iXRD system by PROTO Company, a MG40 head equipped with a 2-mm diameter collimator and following the conditions used in [11]. Electrolytic etching was applied successively at the same location to perform the measurement at different depths. Surface roughness was also measured three times by a conventional stylus type instrument.

2.2. Artificially worn cutting tools

This work focuses on the flank wear as it has already been identified as the most critical wear type affecting residual stress generation [21]. Flank wear can be described by two main parameters: the flank wear length (VB), as well as a flank wear angle (α_{VB}), as shown in Figure 1.

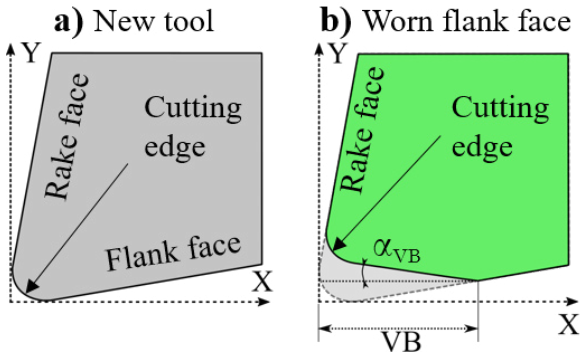

Fig. 1. 2D representation of (a) a new and (b) a worn tool

This description of a worn profile was based on the literature [13,18], which, in some cases, also reported a negative wear angle between the flank face and the machined surface [15].

To validate the numerical methodology, a fully controlled worn tool geometry was needed. Artificially worn tools were manufactured using an NC grinding machine [22]. The tool path and grinding wheel orientation were carefully programmed to create different VB flank wear levels, keeping a flank wear angle within the range of 16 to 17°.

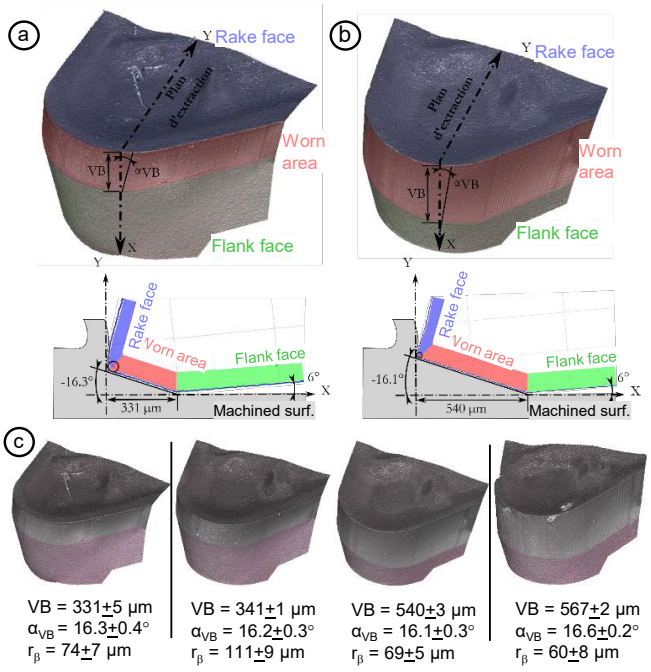

Fig. 2. Artificially worn tool geometries: example of 3D topography and local tool profile (a) with a 331µm and (b) 540µm VB flank wear, (c) detailed geometrical features of the 4 generated tools (3D scans performed before the cutting edge preparation).

A cutting edge preparation technique was then applied to control the cutting edge radius. The resulting 3D worn geometries were precisely analysed using an ALICONA focus-variation microscope to extract the different geometrical features such as the flank wear length, wear angle (Fig. 1a,b). or cutting edge radius (Fig. 1c). This process was applied to generate several inserts and 4 artificially worn tools covering two different wear states were specifically selected (Fig.1 c), in addition to the new inserts. The different cutting edge radius values are described in the Table 1.

Table 1. Evolution of the cutting edge radius before grinding and after edge preparation

Wear level 1	VB 331 µm	VB 341 µm
After grinding	24±9 µm	19±7 µm
After edge preparation	74±7 µm	111±9 µm
Wear level 2	VB 540 µm	VB 567 µm
After grinding	19±5 µm	16±2 µm
After edge preparation	69±5 µm	60±8 µm

Contrary to an experimental worn tool, where the geometry of the flank wear face can be irregular along the tool tip and also complex, on these tools, the wear is constant along the cutting edge and exhibits a simple geometry. This type of pattern can be easily reproduced in a numerical simulation, which was the objective of this preparation process.

Regarding the two wear levels, the wear angle (αVB) could be considered as large compared to what can be observed in the literature. However, some experimental works highlighted that an angle of this magnitude can be observed [15].

3. Modelling approach

3.1. General concept

The proposed work builds upon the early developed hybrid method to predict the residual stresses and the really last works related to surface integrity [24,25].

The prediction of the residual stresses is achieved by applying equivalent thermomechanical loadings into a Finite Element (FE) model of the machined surface. The 3D stationary stress distribution is computed following three keys steps: 1) the decomposition of the actual 3D problem into elementary 2D sections, 2) the computation of the thermomechanical loadings generated by each sections onto the machined surface and 3) the simulation of the mechanical stress state induced by the merged equivalent loadings after several revolutions and ultimately, the extraction of the residual stress profile at a given location.

3.2. Geometrical decomposition of the 3D problem

The first step is to decompose the 3D problem from a geometrical point of view. A geometrical model (Fig. 3b) of the actual 3D turning configuration (Fig. 3a) is built and used to identify the corresponding cut section (Fig. 3c). The latter can obviously vary depending on the tool geometry, tool holder and tool path. The cutting edge is then discretised and several perpendicular cutting planes are defined all along the cutting zone They provide the local tool geometry as well as the corresponding local uncut chip thickness *h(i)* (Fig. 3d).

It is important to emphasise that the exact tool geometry is considered, meaning the exact local worn tool profile including the local rake angle, flank wear level and edge rounding. It is thus possible to use any worn tool geometry and import properly selected sections into the numerical methodology.

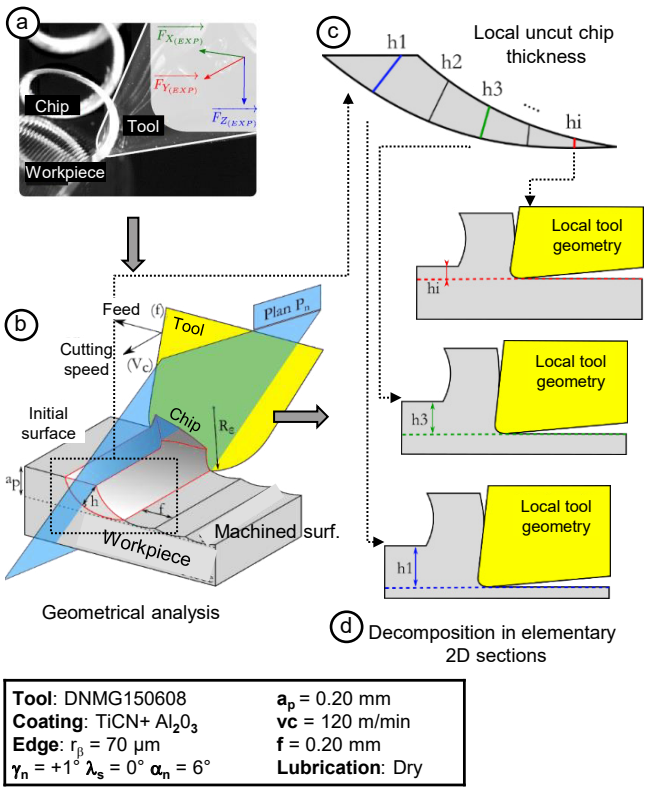

Fig. 3. Segmentation procedure of the 3D problem: (a) investigated configuration, (b) geometrical model, (c) identification of the cutting section, (d) decomposition in elementary 2D sections considering the local tool geometry and corresponding uncut chip thickness

3.3. Modelling of the thermomechanical loadings

Each of the extracted section is then imported into a 2D orthogonal cutting model. 2D thermomechanical simulations are conducted within an explicit framework using an Arbitrary Lagrangian Eulerian formulation (ALE). One of the key benefits of the approach is that it allows for each section to be simulated separately using parallel computing (Fig. 4a).

A Johnson-Cook flow stress model identified by Mondelin et al. [20] has been used to model the 15-5 PH mechanical behaviour (Table 2, Eq.1.).

Table 2. Johnson-Cook's parameters of the 15-5 PH

A [MPa]	B [MPa]	n	m	C	$\dot{\varepsilon}_0$	T_F [°C]	T_0 [°C]
855	448	0,14	0.63	0,0137	0.001	1440	20

$$\sigma_{eq} = \left[A + B \cdot \left(\bar{\varepsilon_p}\right)^n\right] \cdot \left[1 + C \cdot \ln\left(\frac{\dot{\varepsilon_p}}{\dot{\varepsilon_0}}\right)\right] \cdot \left[1 - \left(\frac{T - T_0}{T_F - T_0}\right)^m\right] \quad (1)$$

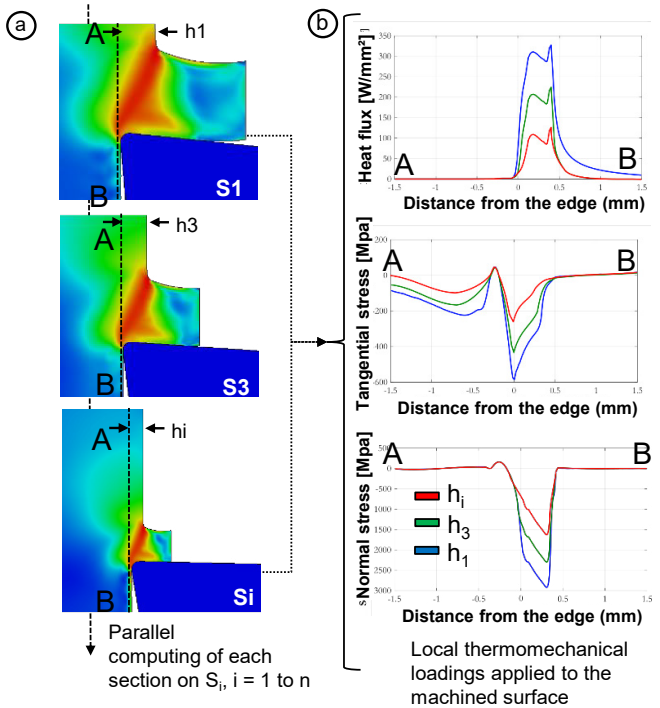

Fig. 4. Segmentation procedure of the 3D problem: (a) 2D ALE simulation of each section and (b) extraction of the simulated local thermomechanical loadings withstood by the machined surface.

A master (tool) / slave (workpiece) penalty contact method as well as tribologically identified friction and heat partition models were implemented. The thermal conductance between the tool and the workpiece is 10^4 W/m^2.K.

The interested reader will be able to find all the details and input data in [20,25].

Thermomechanical loadings withstood by the machined surface are extracted along a path (A-B dotted black line in Fig. 4a), consisting in the really last element layer. Three major outputs are considered in these simulations: the heat flux density, the normal stress and tangential stress evolutions along this path. The Figure 4b shows some example results for three different sections, i.e. three different local tool geometries and uncut thicknesses, with the amplitude of the three loadings increasing as h increases. Finally, a calibration step is applied based on the experimentally recorded machining forces and the combined numerical ones in order to adjust the magnitude of the equivalent thermomechanical loadings [25].

3.4. Simulation of the residual stresses

The 2D loading profiles previously simulated for each section (Fig. 4b) are then merged in order to generate the equivalent 3D thermomechanical loadings (Fig. 5a) to be applied in the macroscopic 3D model (Fig. 5b). The Figure 5b illustrates the resulting loadings, which are further moved along the cutting direction in the FE model according to the cutting speed for a single revolution. As only an elementary representative volume is modelled, a proper cutting time but also a consistent cooling phase considering the whole revolution of the workpiece are calculated and implemented.

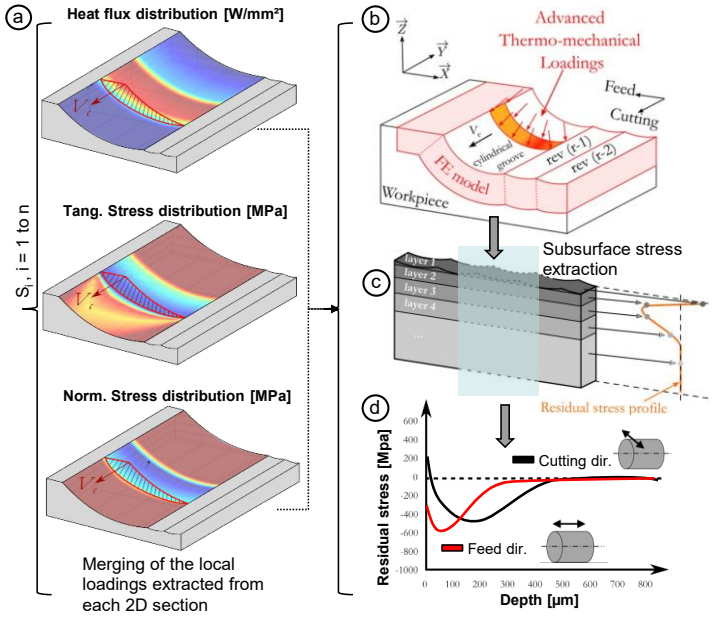

Fig. 5. Hybrid simulation method to 3D predict the residual stress distribution: (a) assembling of the 2D loadings to build a 3D loading distribution, (b) implicit 3D FE model with the corresponding loadings, (c) extraction method to generate the stress profile and (d) example of simulated residual stress profiles in the cutting and feed directions.

In order to simulate several revolutions and reach a steady state, the model geometry has to be updated every two revolutions due to the material removal. A new geometry of the machined surface and corresponding mesh are then generated and a transfer of the residual stress fields is carried out from the previous mesh towards the new meshed geometry. Moreover, to take into account the cyclic behaviour of the machined material, a von Mises elastoplastic behaviour associated with an Armstrong-Frederick kinematic hardening is implemented in this model [20] (Table 3).

Table 3. Coefficients of the Armstrong-Frederick model

Temperature [°C]	*σy [MPa]*	*C*	*γ*
20	530	421.405	730
300	382	284.420	508
600	197	120.000	600

The simulation of 7 revolutions for one configuration was achieved in 24h of CPU time with a 3.2 GHz processor (4 cores).

Finally, the numerical residual stresses are extracted layer by layer along the depth, and averaged along the feed direction corresponding to several revolutions (Fig. 5c) so as to extract a single residual stress value at a corresponding depth beneath the surface, providing the predicted residual stress profile (Fig. 5d).

5. Results and discussion

The whole methodology was thus applied to the case study described in Section 2. The 3D geometries of the 5 investigated configurations were decomposed into 6 elementary 2D sections. The artificially generated wear being homogeneous all along the cutting zone, the average VB flank wear length, angle and edge radius (Fig. 2c) were considered and applied to each of the elementary 2D sections.

The predicted residual stress gradients in the feed and cutting directions are presented in the Figures 6 and 7 and compared to the experimental ones. The latter are plotted as envelopes combining the residual stress profiles for the two similar wear levels.

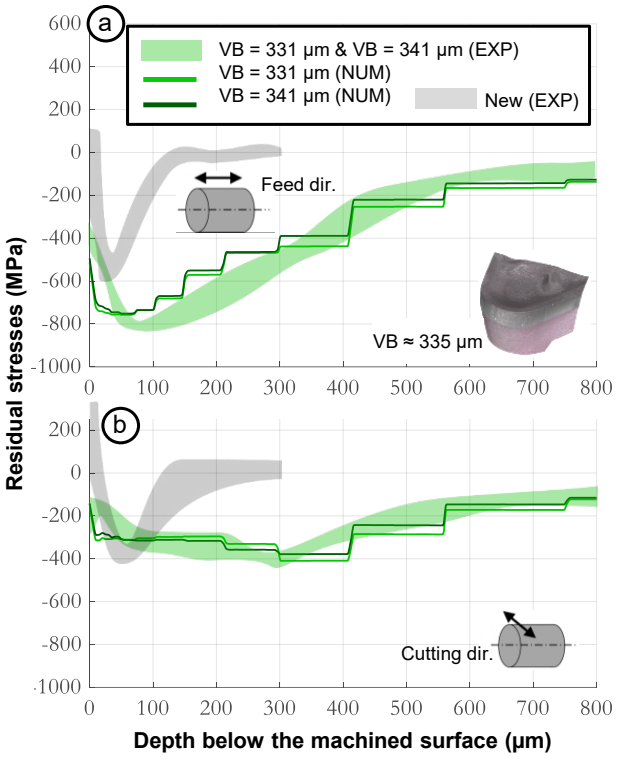

Fig. 6. Comparison between the experimental (EXP) and numerical (NUM) data for the first wear level and a new (NEW) tool: (a) residual stresses in the feed direction and (b) cutting direction

Turning with a moderate or high flank wear is found to induce a more compressive state, which is consistently predicted by the numerical approach. With a VB of 331µm and 341µm (Fig. 6a), the predicted surface residual stress in the feed direction is slightly more compressive (+25%) but the high surface roughness (Ra ≈ 3µm) could affect the quality of the XRay measurements especially along this direction. The maximum compressive stress is reduced by 10% (Fig. 6a) while the simulated affected depth is consistent.

With a VB of 540µm and 567µm (Fig. 7a), the numerical prediction does not fully agree with the numerical results over the first 50µm. The surface residual stress is highly compressive (+200%) whereas the stress profile beyond 100µm remains consistent.

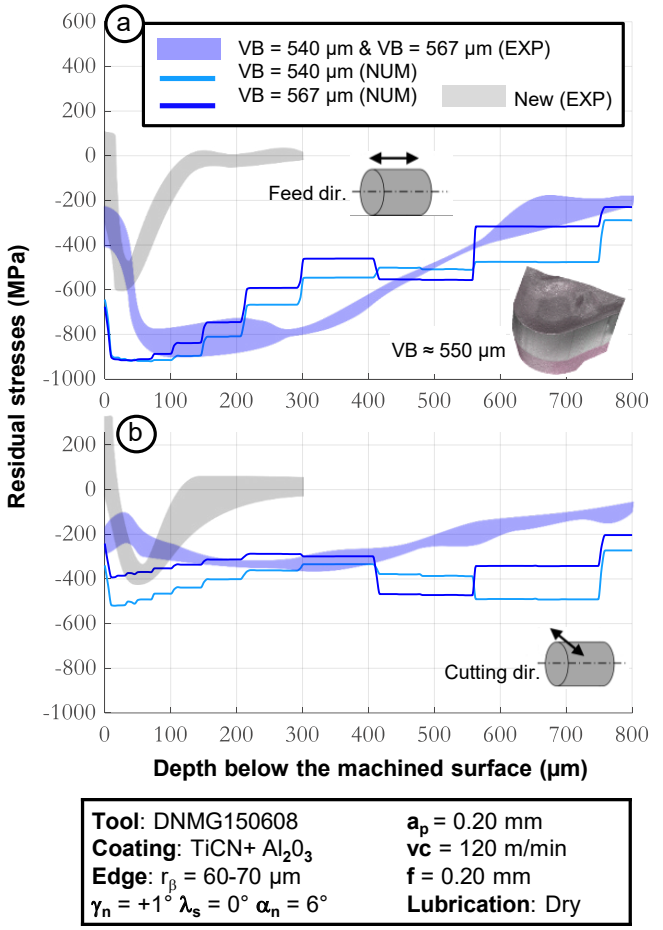

Fig. 7. Comparison between the experimental (EXP) and numerical (NUM) data for the second wear level and a new (NEW) tool: (a) residual stresses in the feed direction and (b) cutting direction

In the cutting direction (Figs. 6b and 7b), the numerical results are in relative good agreement, only the maximum compressive stress with the highest wear level appears overestimated (+43%). This could be connected to a potential subsurface material transformation and should be further investigated.

Conclusions

This paper has presented a numerical approach to predict the drift of the residual stress state induced by wear in turning.

The 3D cutting configuration is discretized into 2D elementary sections subsequently simulated in a thermomechanical FE model to identify the local loadings. The latter are then merged and calibrated to generate the 3D boundary conditions of a macroscopic model able to simulate the residual stress state after several revolutions.

Longitudinal turning tests have been carried out with new and artificially worn inserts in order to assess the impact of a worn geometry on the residual stresses.

The proposed method led to promising results which proved its consistency, even if some limitations should be further investigated as far as the top surface residual stress is concerned.

As a perspective, the proposed methodology could be easily applied to complex worn tool geometries, i.e. with a varying wear level all along the cutting edge. The next steps are now to adapt this approach to normal experimental worn tool with an inconsistent and complex wear geometry but also to predict residual stress profiles for continuously progressing tool wear.

Acknowledgements

Authors would like to express their gratitude to AIRBUS HELICOPTERS, FRAMATOME, SAFRAN, CETIM and the French National Research Agency (ANR) for their financial support or contribution within the framework of the ANR Industrial Chair MISU (ANR-19-CHIN-003).

References

[1] Rech, J., Hamdi, H., Valette, S., 2008, Rédaction du chapitre 3 dénommé “Surface finish and integrity”, Titre de l’ouvrage édité par J. Paulo Davim : « Machining : fundamentals and recent advances », Springer 2. London: Springer London.

[2] Smith, S., Melkote, S. N., Lara-Curzio, E., Watkins, T. R., Allard, L., et al., 2007, Effect of surface integrity of hard turned AISI 52100 steel on fatigue performance, Materials Science and Engineering A, DOI:10.1016/j.msea.2007.01.011.

[3] Jawahir, I. S., Brinksmeier, E., M’Saoubi, R., Aspinwall, D. K., Outeiro, J. C., et al., 2011, Surface integrity in material removal processes: Recent advances, CIRP Annals - Manufacturing Technology, DOI:10.1016/j.cirp.2011.05.002.

[4] Guo, Y. B., Warren, A. W., Hashimoto, F., 2010, The basic relationships between residual stress, white layer, and fatigue life of hard turned and ground surfaces in rolling contact, CIRP Journal of Manufacturing Science and Technology, DOI:10.1016/j.cirpj.2009.12.002.

[5] Yang, X., Liu, C. R., Grandt, A. F., 2002, An experimental study on fatigue life variance, residual stress variance, and their correlation of face-turned and ground Ti 6Al-4V samples, Journal of Manufacturing Science and Engineering, Transactions of the ASME, 124/4:809–819, DOI:10.1115/1.1511174.

[6] Hua, J., Umbrello, D., Shivpuri, R., 2006, Investigation of cutting conditions and cutting edge preparations for enhanced compressive subsurface residual stress in the hard turning of bearing steel, Journal of Materials Processing Technology, 171/2:180–187, DOI:10.1016/j.jmatprotec.2005.06.087.

[7] Dahlman, P., 2004, The influence of rake angle, cutting feed and cutting depth on residual stresses in hard turning, Journal of Materials Processing Technology, 147:181–184, DOI:10.1016/j.matprotec.2003.12.014.

[8] Outeiro, J. C., Pina, J. C., M’Saoubi, R., Pusavec, F., Jawahir, I. S., 2008, Analysis of residual stresses induced by dry turning of difficult-to-machine materials, CIRP Annals - Manufacturing Technology, 57/1:77–80, DOI:10.1016/j.cirp.2008.03.076.

[9] Caruso, S., Umbrello, D., Outeiro, J. C., Filice, L., Micari, F., 2011, An experimental investigation of residual stresses in hard machining of AISI 52100 steel, Procedia Engineering, 19:67–72, DOI:10.1016/j.proeng.2011.11.081.

[10] Matsumoto, Y., Hashimoto, F., Lahoti, G., 1999, Surface Integrity Generated by Precision Hard Turning. Annals of the CIRP vol.48, p. Annals of the CIRP vol.48, 59-62.

[11] Chandrasekaran, H., M’Saoubi, R., Högman, B., Nordh, L. G., Coulon, B., et al., 2005, Development of machinability enhanced tool steels for improved product economy in hard milling. .

[12] Liu, M., Takagi, J. I., Tsukuda, A., 2004, Effect of tool nose radius and tool wear on residual stress distribution in hard turning of bearing steel, Journal of Materials Processing Technology, 150/3:234–241, DOI:10.1016/j.jmatprotec.2004.02.038.

[13] Chen, L., El-Wardany, T. I., Harris, W. C., 2004, Modelling the effects of flank wear land and chip formation on residual stresses, CIRP Annals - Manufacturing Technology, 53/1:95–98, DOI:10.1016/S0007-8506(07)60653-2.

[14] Tonshoff, H. K., Arendt, C., Ben Amor, R., 2000, Cutting of hardened steel, CIRP Annals - Manufacturing Technology, 49/2:547–566, DOI:10.1016/S0007-8506(07)63455-6.

[15] Ducobu, F., Arrazola, P. J., Rivière-Lorphèvre, E., Filippi, E., 2015, Finite element prediction of the tool wear influence in Ti6Al4V machining, in *Procedia CIRP*.

[16] Madariaga, A., Kortabarria, A., Hormaetxe, E., Garay, A., Arrazola, P. J., 2016, Influence of Tool Wear on Residual Stresses When Turning Inconel 718, Procedia CIRP, 45:267–270, DOI:10.1016/j.procir.2016.02.359.

[17] Liu, Y., Xu, D., Agmell, M., Saoubi, R. M., Ahadi, A., et al., 2021, Numerical and experimental investigation of tool geometry effect on residual stresses in orthogonal machining of Inconel 718, Simulation Modelling Practice and Theory, 106/June 2020:102187, DOI:10.1016/j.simpat.2020.102187.

[18] Muñoz-Sánchez, A., Canteli, J. A., Cantero, J. L., Miguélez, M. H., 2011, Numerical analysis of the tool wear effect in the machining induced residual stresses, Simulation Modelling Practice and Theory, 19/2:872–886, DOI:10.1016/j.simpat.2010.11.011.

[19] Liang, X., Liu, Z., Wang, B., Song, Q., Cai, Y., et al., 2021, Prediction of residual stress with multi-physics model for orthogonal cutting Ti-6Al-4V under various tool wear morphologies, Journal of Materials Processing Technology, 288/August 2020:116908, DOI:10.1016/j.jmatprotec.2020.116908.

[20] Mondelin, A., Valiorgue, F., Rech, J., Coret, M., Feulvarch, E., 2012, Hybrid model for the prediction of residual stresses induced by 15-5PH steel turning, International Journal of Mechanical Sciences, 58/1:69–85, DOI:10.1016/j.ijmecsci.2012.03.003.

[21] Clavier, F., Valiorgue, F., Courbon, C., Dumas, M., Rech, J., et al., 2020, Impact of cutting tool wear on residual stresses induced during turning of a 15-5 PH stainless steel, Procedia CIRP, 87:107–112, DOI:10.1016/j.procir.2020.02.074.

[22] Clavier, F., Valiorgue, F., Courbon, C., Rech, J., Pascal, H., et al., 2022, Experimental analysis of the impact of an artificially generated tool wear pattern on the residual stress induced by 15-5PH steel turning, Procedia CIRP, 108:394–399, DOI:10.1016/j.procir.2022.04.075.

[23] Valiorgue, F., Rech, J., Hamdi, H., Gilles, P., Bergheau, J. M., 2012, 3D modeling of residual stresses induced in finish turning of an AISI304L stainless steel, International Journal of Machine Tools and Manufacture, 53/1:77–90, DOI:10.1016/j.ijmachtools.2011.09.011.

[24] Methon, G., Valiorgue, F., Dumas, M., Van-Robaeys, A., Masciantonio, U., et al., 2019, Development of a 3D hybrid modeling of residual stresses induced by grooving, Procedia CIRP, 82:400–405, DOI:10.1016/j.procir.2019.04.002.

[25] Dumas, M., Fabre, D., Valiorgue, F., Kermouche, G., Van Robaeys, A., et al., 2021, 3D numerical modelling of turning-induced residual stresses – A two-scale approach based on equivalent thermo-mechanical loadings, Journal of Materials Processing Technology, 297/June, DOI:10.1016/j.jmatprotec.2021.117274.